Shear model for URM walls retrofitted with FRP

M.A. ElGawady,

Auckland University, New Zealand

2005 NZSEE Conference

ABSTRACT: This paper presents an analytical model for in-plane shear behavior of unreinforced masonry (URM) walls retrofitted using fibre-reinforced polymers (URM-FRP). The proposed model idealises masonry, epoxy, and FRP in a URM-FRP as different homogenous layers. Then, using principles from the theory of elasticity, the governing differential equation of the system is formulated and solved. A simple computer program was developed to combine the solution of the differential equations with material nonlinearity. The material nonlinearity was represented by step-by-step layer stiffness degradation; after each step, the equations are resolved linearly. The proposed basic analytical model allows the fundamental investigation of in-plane shear behaviour of URM-FRP. Finally, effects of epoxy and masonry allowable shear stresses and FRP axial rigidity on the shear strength of URM-FRP are examined. In addition, comparisons with three existing models are carried out.

1 INTRODUCTION

FRP provides a promising technique for retrofitting of seismically inadequate URM walls. However, limited design proposals for the shear strength of URM-FRP have been made (Triantafillou 1998, Triantafillou and Antonopoulos 2000, ICBO 2001). In these proposals, the following expression is used to evaluate the shear strength (F) of an URM-FRP:

$$F = F_m + F_{FRP} \tag{1}$$

where F_m = shear strength of URM wall ; F_{FRP} = contribution of FRP to the shear strength of URM wall. The main difference between available proposals lies in the evaluation of F_{FRP}. In the case of FRP applied perpendicularly to the longitudinal member axis in a single-side to a URM wall, the models are briefly discussed. Triantafillou (1998) proposed the following equation for F_{FRP}

$$F_{FRP} = \rho_h E_{FRP} \varepsilon_{eff} t L \tag{2}$$

where ρ_h = reinforcement ratio (area fraction) of FRP in the horizontal direction; E_{FRP} = modulus of elasticity of FRP, t = thickness of masonry wall ; L = length of masonry wall ; ε_{eff} = effective strain of FRP at failure, and can be calculated as follows:

$$\varepsilon_{eff} = 0.0119 - 0.0205(\rho_h E_{FRP}) + 0.0104 (\rho_h E_{FRP})^2 \qquad 0 \le \rho_h E_{FRP} \le 1\text{GPa} \tag{3a}$$

$$\varepsilon_{eff} = 0.00245 - 0.00065(\rho_h E_{FRP}) \qquad \rho_h E_{FRP} > 1\text{GPa} \tag{3b}$$

Later on, Triantafillou and Antonopoulos (2000) calculated the effective strains as the minimum of:

$$\varepsilon_{eff} = 0.00065 \left(\frac{f_c^{\frac{2}{3}}}{\rho_h E_{FRP}} \right)^{0.56} \qquad (\text{debonding}) \tag{4a}$$

$$\varepsilon_{eff} = 0.17\left(\frac{f_c^{\frac{2}{3}}}{\rho_h E_{FRP}}\right)^{0.30} \varepsilon_{FRP} \text{ for CFRP and } 0.048\left(\frac{f_c^{\frac{2}{3}}}{\rho_h E_{FRP}}\right)^{0.47} \varepsilon_{FRP} \text{ for AFRP (rupture)} \quad (4b)$$

where f_c = concrete characteristic compressive strength. To transfer the mean value of ε_{eff} to a characteristic value, the expressions in Equation 4 should be multiplied by a reduction factor of 0.8. In addition, the characteristic value of ε_{eff} has an upper limit of 0.005.

AC125 of ICBO [9] uses the following expression for FFRP:

$$F_{FRP} = 0.75\rho_h f_j t L \quad \text{and} \quad f_j = 0.004 E_{FRP} \le 0.75 f_{FRP,u} \quad (5)$$

where f_j = axial force in FRP; $f_{FRP,u}$ = ultimate tensile strength of FRP.

The main drawback of Equations 3 and 4 is that the axial strain in FRP is estimated based on empirical function formulated based on tests of reinforced concrete shallow beams. The main drawback of Equation 5 is that a constant strain value of 0.004 is assumed for axial strain in FRP, regardless of its axial rigidity. This is controversial to what with respect was observed during experimental events. Finally, these models (Triantafillou models and AC125 model) add the contribution of FRP (F_{FRP}) to the shear strength of URM wall (F_m) maintaining an unchanged F_m; this aspect should be revised since a recent investigation (ElGawady 2004) shows that it is not the case.

2 NEW SHEAR STRENGTH MODEL

This section presents an innovative shear model for URM-FRP. The model idealises masonry, epoxy, and FRP in a single–sided, retrofitted URM using FRP as different layers (Figure 1) with isotropic homogenous elastic materials. Then, the governing differential equation of the system is formulated.

2.1 Derivation of governing equations

The differential element in Figure 2 shows the in-plane shear stresses acting on the masonry (τ_{xy}^m) and FRP (τ_{xy}^f), as well as the two components of the epoxy shear stress (τ_{zx}^e, τ_{zy}^e). The model assumes that: 1) forces are transferred from the masonry wall to FRP through shear only; 2) epoxy carries only surface stresses; 3) both masonry and FRP layer carry only in-plane shear stresses; 4) no dowel action; the applied lateral forces are applied uniformly over the wall cross-section; 5) finally, the effect of asymmetry (due to applying FRP on single side) is neglected. From Figure 2 and by using equilibrium equations and principles from elasticity, the following equation can be written:

$$t^f \nabla^2 \tau_{xy}^f - \frac{G^e}{t^e}\frac{\tau_{xy}^f}{G^f} + \frac{G^e}{t^e}\frac{\tau_{xy}^m}{G^m} = 0 \quad (1)$$

where G^e, G^m, and G^f = epoxy, masonry, and fibre shear modulus respectively; t^e, t^m t^f, = epoxy, masonry, and fibre thickness respectively. In addition, the relationship between the external applied shear force/unit length of the wall N_{xy} and the in-plane shear stresses can be written as follows:

$$N_{xy} = \tau_{xy}^m t^m + \tau_{xy}^f t^f \quad (2)$$

Substitute for $\tau_{xy}{}^m$ from Equation 2 into Equation 1 and divide by t^f, then:

$$\nabla^2 \tau_{xy}^f - \lambda^2 \tau_{xy}^f + C_o = 0 \quad (3)$$

where $C_o = \frac{N_{xy}}{t^e t^m t^f}\frac{G^e}{G^m}$, $\lambda^2 = \left(\frac{G^e}{t^e}\right)\left(\frac{1}{t^f G^f} + \frac{1}{t^m G^f}\right)$

Using similar procedure for laboratory joints analysis, Kim and Kedward (2001) proposed the following double Fourier sine series as the solution of such differential equation:

$$\tau^{f}_{xy} = \sum_{m=1}^{\infty}\sum_{n=1}^{\infty} \frac{C_{mn}}{\left(\frac{m\pi}{L}\right)^2 + \left(\frac{n\pi}{h}\right)^2 + \lambda^2} \sin\frac{m\pi x}{L} \sin\frac{n\pi y}{h} \qquad (4)$$

where $C_{mn} = \frac{4}{Lh}\int_0^a\int_0^b C_o \sin\frac{m\pi x}{L}\sin\frac{n\pi y}{h}\,dx\,dy$

This solution satisfies both the governing differential equation and the assumed boundary conditions (i.e. $\tau^{f}_{xy} = 0$ at all the FRP boundaries). Then, the shear resultant in the epoxy layer is as follows:

$$\tau_{epoxy} = \sqrt{\left(\sum_{m=1}^{\infty}\sum_{n=1}^{\infty} A_{mn}\pi m\, t^{f} \cos\frac{m\pi x}{L}\sin\frac{n\pi y}{h}\right)^2 + \left(\sum_{m=1}^{\infty}\sum_{n=1}^{\infty} A_{mn}\pi n\, t^{f} \sin\frac{m\pi x}{L}\cos\frac{n\pi y}{h}\right)^2} \qquad (5)$$

the contribution of the FRP to the shear force can be calculated as follows:

$$F_{FRP} = \tau^{f}_{xy}\, t^{f}\, L \qquad (6)$$

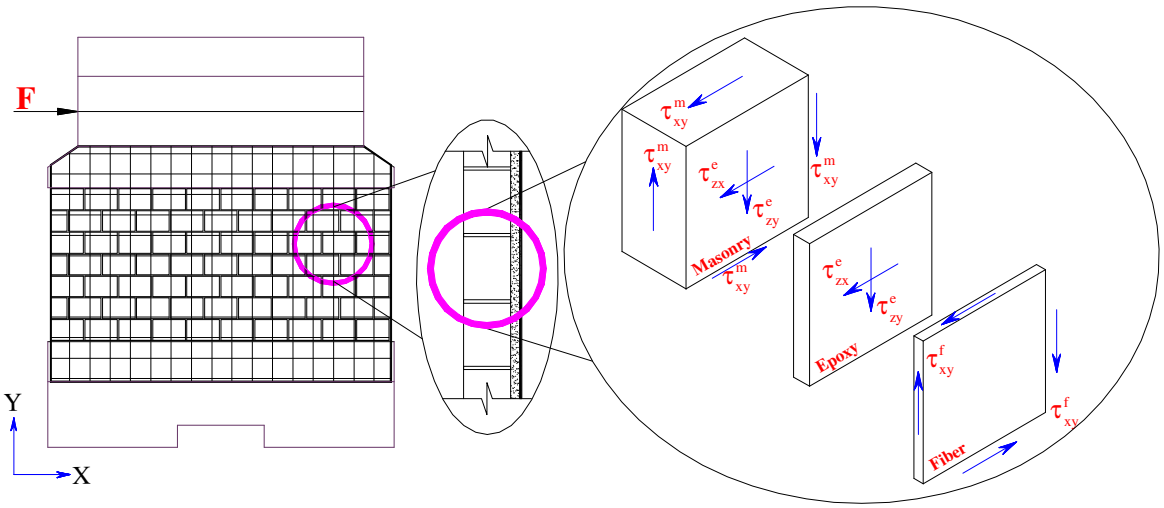

Figure 1. Single sided URM-FRP and differential element of the same retrofitted wall

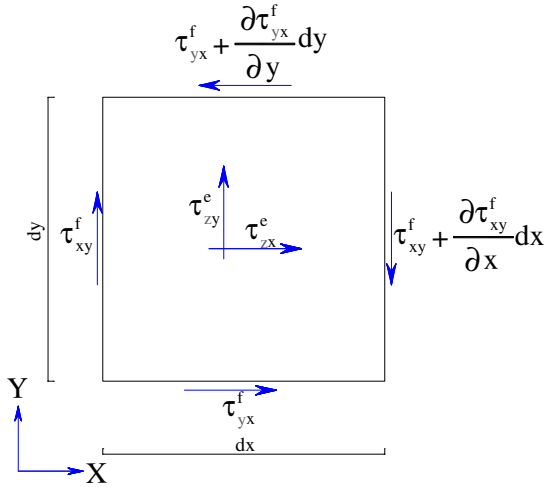

Figure 2. Shear stresses acting on an element of the inner surface FRP layer

Finally, the shear force and stresses resisted by the masonry can be calculated as follows:

$$\tau_{xy}^{m} = \frac{F - F_{FRP}}{Lt} \tag{7}$$

2.2 **Non-linear Shear Analysis of a URM-FRP**

The equations presented in the previous section can be used to model the linear shear behaviour of URM-FRP. To take into consideration the nonlinearity of the materials, a step-by-step stiffness degradation of masonry as well as epoxy has been implemented in a program (Figure 3) written in MATLAB (2002). Note that URM and epoxy layers were assumed to have elastic/perfectly-plastic force-deformation curves, while the FRP layer behaves linearly up to failure (ElGawady 2004).

3 **PARAMETRIC STUDY**

The model has been used to reproduce the shear strength of six URM walls which were retrofitted with FRP on a single side (ElGawady 2004). In general, the comparisons were satisfactory. In this paper, the main purpose is to examine the global shear behavior of URM-FRP or, in other words, to examine: 1) the phenomenon of using effective strain rather than the ultimate strain in the FRP; in addition, examine if this effective strain is a constant value (i.e., similar to AC125) or variable (i.e., similar to what was proposed by Triantafillou (199)). 2) the effect of different material parameters (FRP, epoxy, and masonry properties) on the shear strength of URM-FRP. To achieve these goals, for a given URM wall dimensions, the proposed model was compared to the existing models which are presented in this paper. The URM wall dimensions are 1565 mm long, 1000 mm high, and 75 mm thick. These dimensions are similar to the dimensions in an experimental work (ElGawady 2004).

3.1 **Effect of allowable shear stresses**

Three values of epoxy allowable shear stresses were studied: 1.40 MPa (L type), 3.00 MPa (M type), and 6.00 MPa (H type). The effects of applying these epoxy types to different URM walls with different allowable shear stresses have been studied. The URM wall has three different values for allowable shear stresses: 0.25 MPa (L type), 0.50 MPa (M type), and 1.50 MPa (H type). An elastic shear modulus of 0.7 GPa was used for the masonry layer. For the epoxy layer, a value of 1.5 GPa was used as the initial shear modulus based on manufacturer's data. The results are presented in Figures 4 to 6. In these figures, the following abbreviations have been used:

Trian [Tr 98] = Triantafillou model (1998)

[TA 00] = Triantafillou and Antonopoulos model (2000)

AC 125 = AC125 of ICBO (2001) model

ElG_M-E = the proposed model. The ELG abbreviation is followed by two numbers: masonry and epoxy allowable shear, stresses respectively.

Figures 4 and 5 show the comparison between the proposed model and Equation 3. The horizontal axis represents the axial rigidity of the applied FRP (ρE). The vertical axis represents the FRP efficiency (ζ). The FRP efficiency was defined as following: the ratio between the stresses in the FRP due to any amount of FRP axial rigidity (ρE) to the stresses in the FRP due to the lower value of ρE. A lower value of 0.04 GPa was chosen as minimum value for ρE. In general, all the curves have a trend similar to the one given by Equation 3.

Figure 4 shows the comparisons in the case of masonry of Type H. The figure shows that the rate of degradation of ζ is very high for epoxy Types M and L. In addition, for these epoxy types, the difference in ζ degradation rate is negligible. This is due to the fact that for epoxy Type L the limit on epoxy stiffness degradation dominates the URM-FRP behaviour for all amounts of ρE. A similar explanation can be given for the case of epoxy type M. In case of epoxy Type H, the limit on masonry stiffness degradation dominates the URM-FRP shear behaviour until ρE approximately equals

0.14 GPa. For values of ρE less than or equal to 0.14 GPa, the rate of degradation of ζ is very slow. For ρE greater than 0.14 GPa, the limit on epoxy stiffness degradation dominates the URM-FRP shear behaviour with a higher degradation rate of ζ.

For masonry Type L (Figure 5), the degradation rate given by Triantafillou's model seems to be a lower bound for all types of epoxy. For masonry type H, the degradation rate given by Triantafillou's model appears to be an upper bound for all types of epoxy. Based on this note, one can say that the degradation rate given by Equation 3 is close to an average of all the degradation rates given by different epoxy and masonry parameters. This is expected since Triantafillou (1998) developed his model based on curve-fitting for different beams with different material parameters.

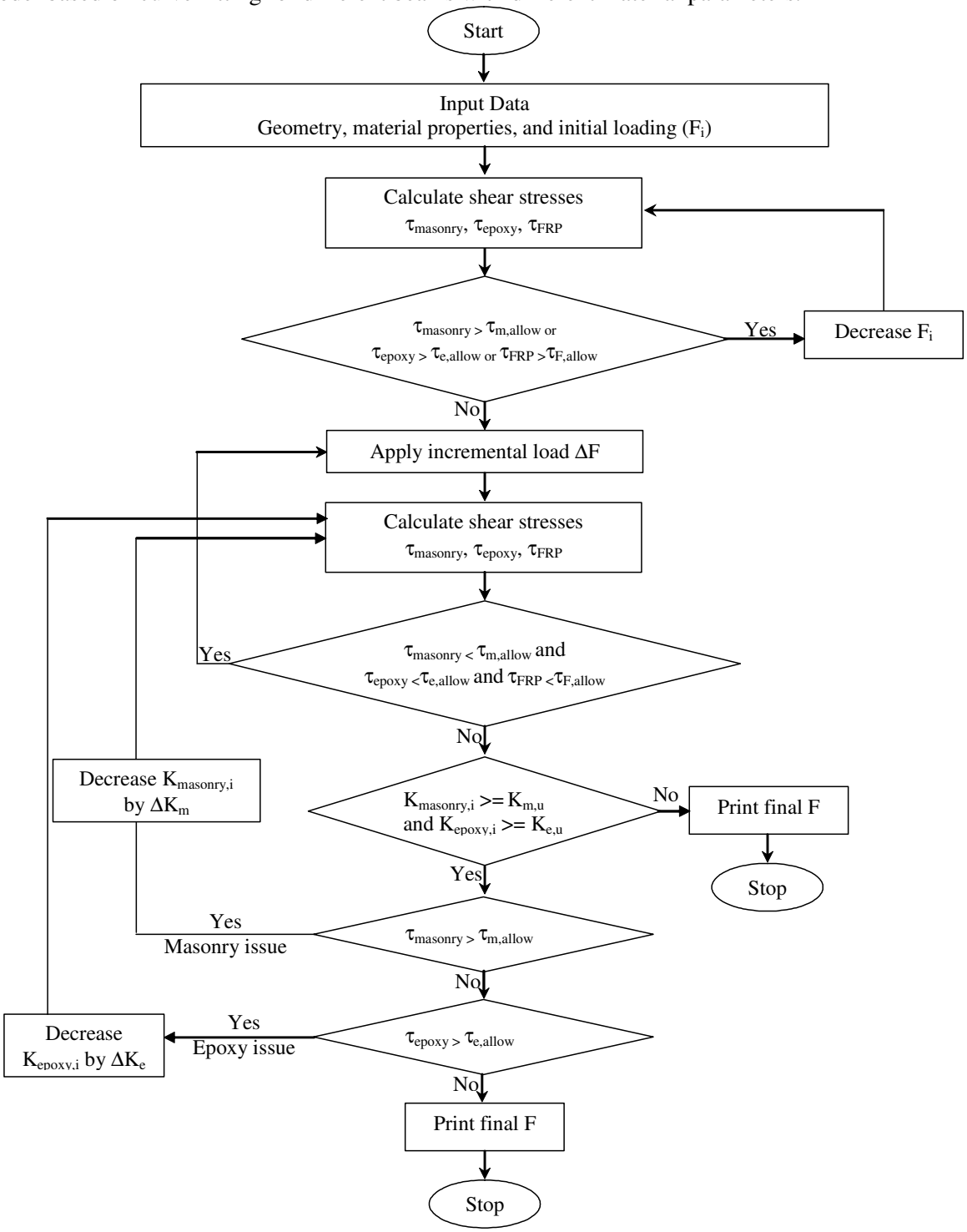

Figure 3 Flow chart for calculating the URM-FRP lateral resistance

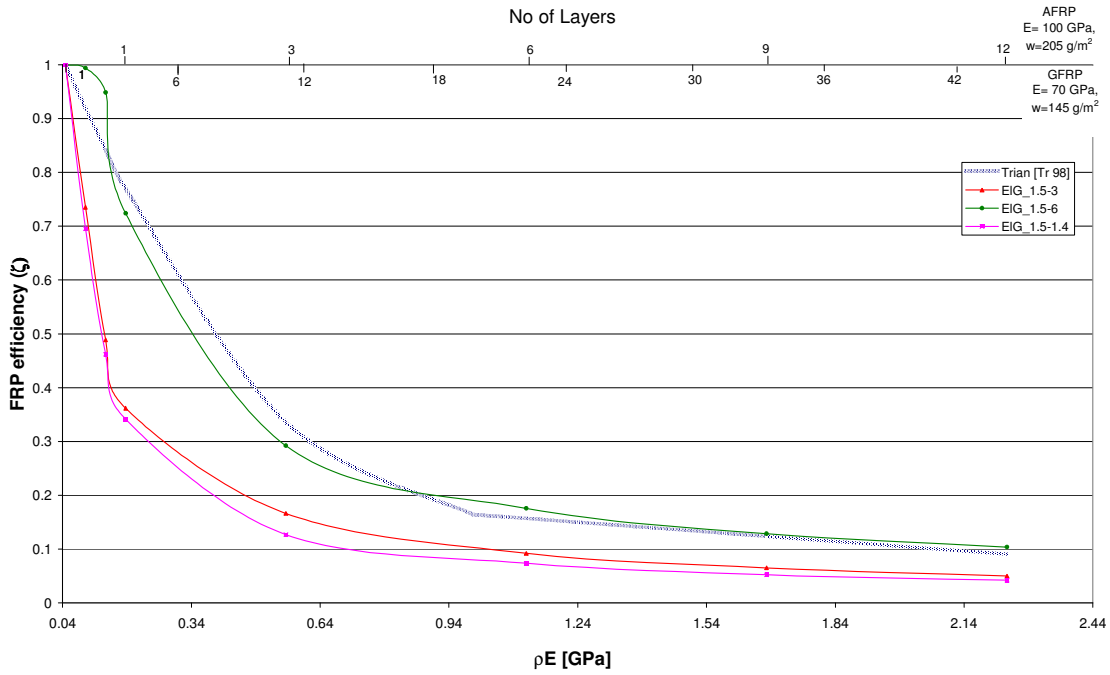

Figure 4 Effect of using type H masonry (1.50 MPa) with epoxy having different allowable shear stresses on FRP efficiency (ζ)

Figures 4 and 5 show that the axial rigidity of the FRP is not the only factor that influences the effective strain in FRP. For all masonry types (L, H), the epoxy type influences the rate of degradation of ζ: the higher the allowable shear stress of epoxy, the lower the rate of degradation of ζ. It appears that when masonry dominates the behavior of URM-FRP, there are less "losses" in FRP effective strain. Finally, careful examination of the figures shows that there are three phases for ζ degradation rate. The first phase when ρE is less than or equal to approximately 0.19 GPa, if epoxy dominates the behaviour, ζ degradation rate is very high. The second phase when ρE is between 0.19 and 1.12 GPa, ζ degradation rate is slower than in the previous phase. In the third phase, when ρE is greater than or equal to 1.12 GPa, ζ degradation rate is very slow and, regardless of the material parameters (except masonry Type L – epoxy Type H), all the efficiency curves are approximately parallel to the curve which comes from Equation 3b. Note that Equation 3 used a value of ρE =1 GPa as the limits between two phases of the degradation rate curve.

Regarding shear strength of URM-FRP, and due to space limitations in this paper, a comparison between the proposed model and the existing model is presented (Figure 6) for the three types of epoxy and for masonry Type H. In general, all the curves tend to be a mix of Equations 3 and 4. However, the absolute values of F are close to the values predicted by Equation 4. Equation 4 seems to be an average of the different F estimated due to different material properties. The divergence between the estimated F by the proposed model and Equation 4 is influenced by material properties. In addition, Equation 3 estimated an F higher than the proposed analytical model. The high difference between Equation 3 and the proposed model is expected since Triantafillou is original model implicitly assumes wrapped retrofitting. Recalling that, in case of wrapped retrofitting, FRP rupture is the most probable mode of failure. For all material properties examined here using the proposed model, no FRP fracture happened. Note that, for RC retrofitted using FRP, analysis of all available experimental work in the literature (Bousselham and Chaallal 2004) shows that approximately 96% of failure in case of one-side retrofitting is due to debonding. This ratio reduced to 50% and 0% in case of U-shape and wrapping, respectively. Regarding AC125 (2001), Equation 5 underestimates F for small values of FRP axial rigidity and overestimates F for high values of FRP axial rigidity.

Figure 6 shows that, by increasing epoxy allowable shear stress, the gain in the shear strength increases. Finally, for the same epoxy and masonry allowable shear stresses, by increasing ρE, F increases until a certain upper limit $(\rho E)_{limit}$; beyond this limit, any increment in ρE leads to reduction

in F. The $(\rho E)_{limit}$ is influenced by epoxy and masonry allowable shear stresses. This reduction in F is due to the following: beyond $(\rho E)_{limit}$, URM-FRP reaches the limit on epoxy stiffness degradation too early before the masonry reaches its allowable shear stress. However, after failure of the FRP, the lateral resistance of the URM-FRP reduced to the lateral resistance corresponding to an URM wall.

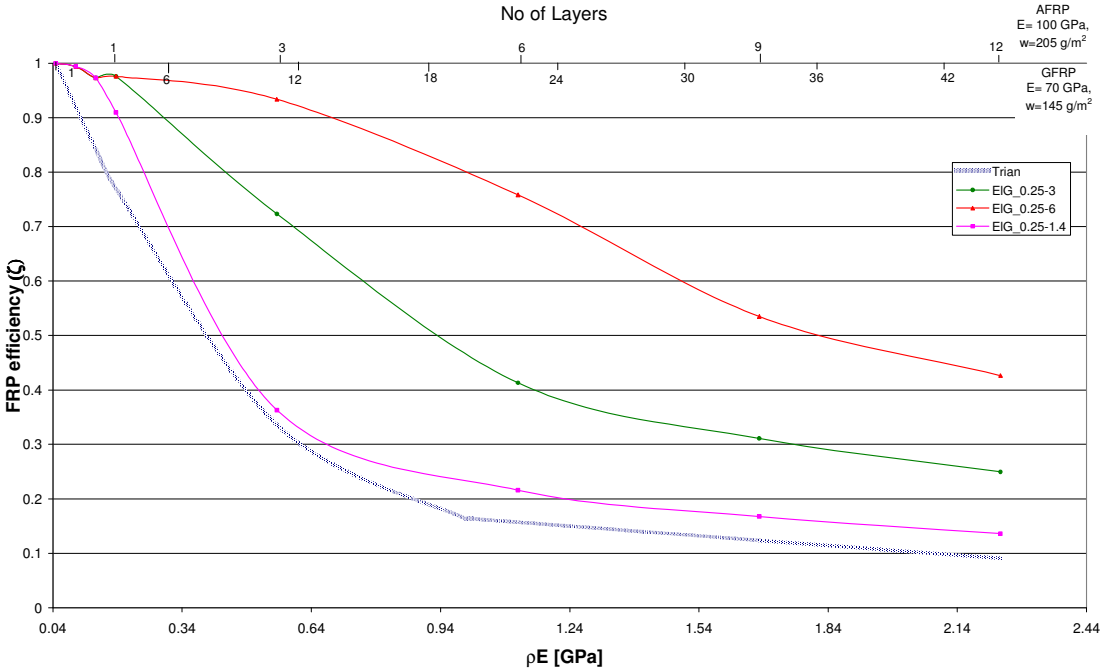

Figure 5 Effect of using L type masonry (0.25 MPa) with epoxy having different allowable shear stresses on FRP efficiency (ζ)

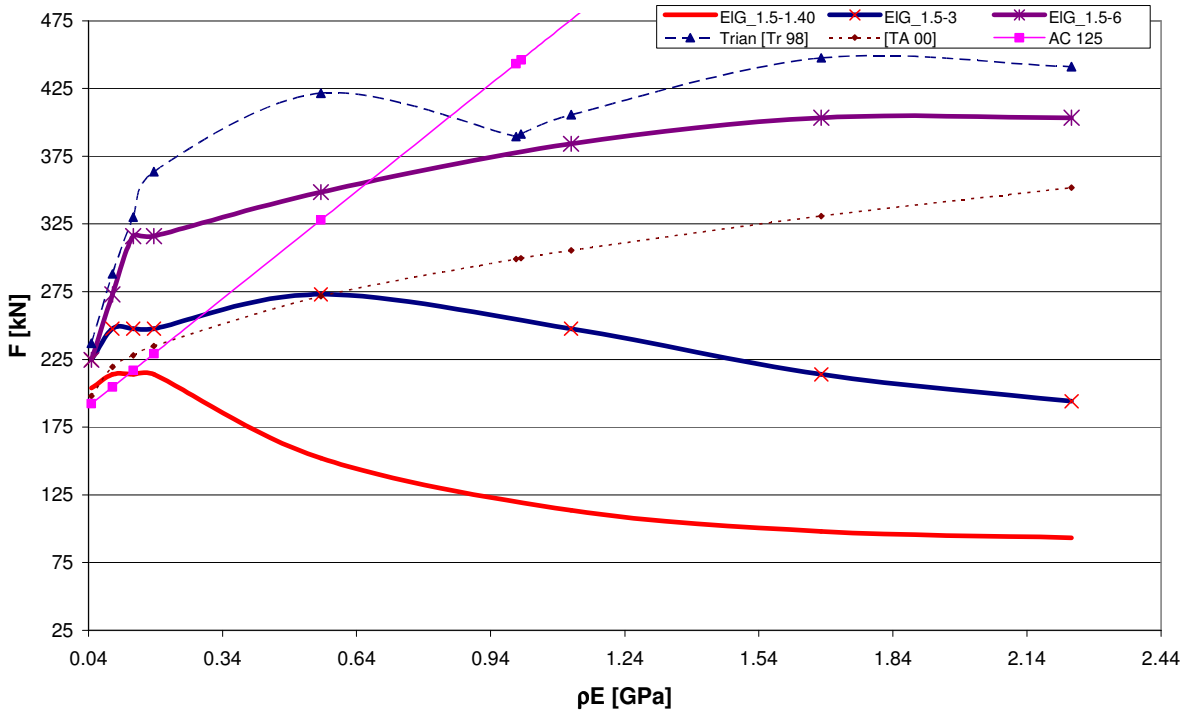

Figure 6. Effect of using H masonry (1.50 MPa) with epoxy having different allowable shear stresses on URM-FRP lateral resistance

The previous remark leads to an important conclusion: using Equation 1 (i.e. when adding masonry lateral resistance to FRP contribution) is correct until a certain limit is reached beyond this limit this equation is no longer valid. To avoid such invalidity in the equation, and in order to have cost-

effective use of FRP, it is proposed to limit $(\rho E)_{limit}$ to a value of 0.19 GPa. For materials properties examined here, this value is smaller than $(\rho E)_{limit}$. For RC beams, Bousselham and Chaallal (2004) observed that beyond a $\rho E/f_c^{0.67}$ of approximately 0.05, F tends to stabilized and they proposed to use such value as a criterion for cost-effective design. If typical values of existing masonry compressive strength are considered (4-7 MPa) with this proposed limit, then the cost-effective design criterion corresponds to a ρE of 0.13-0.17 GPa - which corresponds well to the proposed value estimated by the analytical model.

4 CONCLUSIONS

The results show that the axial strains in FRP are inversely proportional to the FRP axial rigidity as originally proposed by Triantafillou (1998). However, it is not possible to have a single function to represent the relation between ρE and FRP axial strain. The relation between the two quantities depends on several factors (e.g., allowable shear stresses in epoxy and masonry). For high values of ρE (above approximately 1.12 GPa), it is possible to use a single function to describe the relationship between ρE and FRP axial strain.

The higher the allowable shear stresses in epoxy are, the higher F ; the increment in epoxy allowable shear stresses could be achieved by the development of new materials, or by using a mechanical anchorage system at the boundaries. As expected, the effect of such a mechanical anchorage system is higher for high values of ρE.

The proposed model quantifies the relation between F_m and F_{FRP}. The results show that adding F_{FRP} to F_m is only valid until a certain limit. Above this limit, any additional increment in the axial rigidity of FRP has no effect. In other words, there is a threshold with respect to the axial rigidity of the FRP beyond which no increase in shear gain is expected. Such a threshold can be used as a criterion for a cost-effective design. Such a limit on ρE depends on the material allowable stresses and ductility. A value of 0.19 GPa can be proposed as a limit on ρE, which covers the practical values of material properties.

Finally, this research shows that much information is needed to refine characterisations of the materials used in URM-FRP system (i.e., masonry, epoxy, FRP). The proposed model, which describes how URM-FRP behaves due to in-plane loading, can contribute to classifying the needed development.

REFERENCES:

Triantafillou, T. Strengthening of masonry structures using epoxy-bonded FRP laminates. J. Comp. for Constr., ASCE, 2(2), 1998, P. 96-104.

International Conference of Building Officials, AC125. Acceptance criteria for concrete and reinforced and unreinforced masonry strengthened using reinforced-reinforced polymers (FRP), composite systems, 2001.

Triantafillou, T. Antonopoulos, C. Design of concrete flexural members strengthened in shear with FRP. J. Comp. for Constr., ASCE, 4(4), 2000, P. 198-205.

MATLAB Version 6.5.1 (2002). The language of technical computing, the Mathworks Inc

Bousselham, A., Chaallal, O. Shear strengthening RC beams with FRP: assessment of influencing parameters and required research. ACI Struc. J. 101(2), 2004, P. 219-227.

ElGawady, M, Seismic in-plane behaviour of URM walls upgraded with composites. PhD. Thesis, IS-IMAC-ENAC, Swiss Federal Institute of Technology. 2004.

Kim, H., Kedward, K. Stress analysis of in-plane shear loaded adhesively bonded composite joints and assemblies," Office of aviation research, Washington, D.C. Report No. DOT/FAA/AR-017, 2001.

Magenes G., Calvi G. M. In-plane seismic response of brick masonry walls. Earthquake Engineering and Structural Dynamics, 26, 1997, P. 1091-1112.